PHYSICAL REVIEW B **92**, 041302(R) (2015)

Symmetry-induced hole-spin mixing in quantum dot molecules

Josep Planelles,* Fernando Rajadell, and Juan I. Climente
Departament de Química Física i Analítica, Universitat Jaume I, E-12080 Castelló, Spain
(Received 16 March 2015; revised manuscript received 6 May 2015; published 10 July 2015)

We investigate theoretically the spin purity of single holes confined in vertically coupled GaAs/AlGaAs quantum dots (QDs) under longitudinal magnetic fields. A unique behavior is observed for triangular QDs, by which the spin is largely pure when the hole is in one of the dots, but it becomes strongly mixed when an electric field is used to drive it into molecular resonance. The spin admixture is due to the valence-band spin-orbit interaction, which is greatly enhanced in C_{3h} symmetry environments. The strong yet reversible electrical control of hole spin suggests that molecules with C_3-symmetry QDs, like those obtained with [111] growth, can outperform the usual C_2-symmetry QDs obtained with [001] growth for the development of scalable qubit architectures.

DOI: 10.1103/PhysRevB.92.041302 PACS number(s): 73.21.La, 71.70.Ej, 73.40.Gk

Single spins confined in III-V semiconductor quantum dots (QDs) are currently considered as potential qubits for solid-state quantum-information processing, which combine fast optical and electrical manipulation with prospects of scalability [1–4]. In recent years, heavy-hole spin qubits have emerged as a robust and long-lived alternative to electron spins, as they can be less sensitive to dephasing from nuclear spins [1–9]. Significant advances have been reported on hole spin initialization, control, and readout by means of optical excitations [2–4,10–13], and different proposals for electrical control have been put forward [14–18].

Although most works so far have focused on QDs grown along [001], it has been noted that the C_2 point symmetry of such systems gives rise to a splitting of bright exciton states that limits the fidelity of optical hole spin preparation [12,19]. No such splitting is expected, however, in [111] grown QDs due to their higher (C_3) symmetry [20,21], which hence become an alternative worth exploring. Early studies on single (In)GaAs/AlGaAs QDs grown along [111] have revealed that hole states have weak heavy-hole–light-hole (HH-LH) coupling due to the large aspect ratio, which is a prerequisite to obtain pure hole spins and minimize the impact of hyperfine interaction with the lattice nuclei [22]. In turn, magnetophotoluminescence spectra have reported characteristic differences from [001] grown QDs that were ascribed to the influence of the C_3 symmetry on the hole states [23].

In this paper, we move forward and study hole states confined in quantum dot molecules (QDM) formed by a pair of vertically stacked QDs grown along [111]. QDMs present several advantages over single QDs for qubit development, including readout independency from initialization and measurement protocols [24], higher fidelity of spin preparation [10], and enhanced wavelength tunability with external electric fields, which greatly improves prospects of scalability [25]. We consider [111] grown GaAs/AlGaAs QDMs with a triangular shape, similar to those reported in Refs. [26,27], adding longitudinal magnetic and electric fields to control the Zeeman splitting and charge localization. Our calculations show that the HH spin purity is high when the hole is confined in individual QDs, but severe spin admixture takes place when the electric field is used to form molecular orbitals. The spin admixture follows from the formation of orbitals with approximate C_{3h} point group symmetry, which enables otherwise forbidden spin-orbit interactions (SOI). The symmetry-induced SOI does not mix nearby Zeeman sublevels, but it couples bonding and antibonding molecular states split by the tunneling energy. This is in sharp contrast with usual [001] grown QDMs, with C_{2h} symmetry, where tunneling is normally a spin-preserving process [28].

Since the activation of SOI mechanisms is generally associated with a descent of the system symmetry (e.g., system and bulk inversion asymmetry [29], QDM misalignment [30]), the enhancement of SOI for C_3 QDs is apparently counterintuitive. Yet we observe strong spin admixture between hole states over 1 meV apart, which is 2.5 times greater than the largest spin-orbit anticrossing measured in [001] grown QDMs [30]. We provide an explanation through group theory analysis of the multiband $\mathbf{k}\cdot\mathbf{p}$ Hamiltonian for holes, showing this is an exclusive property of C_3 systems, and we discuss the implications of these findings for the development of hole spin qubit architectures.

The Hamiltonian we use to describe hole states reads

$$\mathbb{H} = \mathbb{H}_{\rm BF} + \mathbb{H}_B + \mathbb{H}_{\rm strain} + \{V(\mathbf{r}) + e\,[\phi_{\rm pz}(\mathbf{r}) - F\,z]\}\,\mathbb{I}. \tag{1}$$

Here $\mathbb{H}_{\rm BF}$ is the four-band Burt-Foreman Hamiltonian [31] for [111] grown zinc-blende crystals, which considers HH-LH subband coupling as in the Luttinger model [32] but including position-dependent effective masses. $\mathbb{H}_B$ represents the terms coming from a magnetic field applied along the growth (z) direction. $\mathbb{H}_{\rm strain}$ is the strain Hamiltonian, $V(\mathbf{r})$ is the band-offset potential, e is the hole charge, $\phi_{\rm pz}$ is the piezoelectric potential, F is an axial electric field, and $\mathbb{I}$ is a rank-4 identity matrix. Further details on the Hamiltonian can be found in the Supplemental Material [33]. Hamiltonian (1) is solved numerically after obtaining the strain tensors and piezoelectric fields using the COMSOL package. The eigenstates are Luttinger spinors of the form

$$|n\rangle = \sum_{Jz=-3/2}^{3/2} f^n_{J_z}(\mathbf{r})\,|J=3/2, J_z\rangle, \tag{2}$$

*josep.planelles@uji.es; http://quimicaquantica.uji.es/

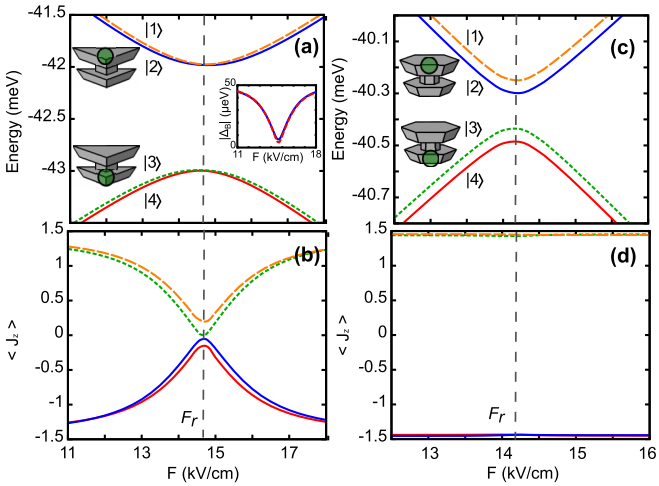

FIG. 1. (Color online) (a) and (b) Hole energy levels and Bloch angular momentum expectation value of a triangular QDM grown along [111], as a function of a vertical electric field. (c) and (d) Same but for a hexagonal QDM. Note the strong spin mixing for triangular QDMs near the resonant field F_r. The structures in (a) and (c) show the hole localization for each doublet. The inset in (a) shows the Zeeman splitting of the upper (solid line) and lower (dashed line) doublet.

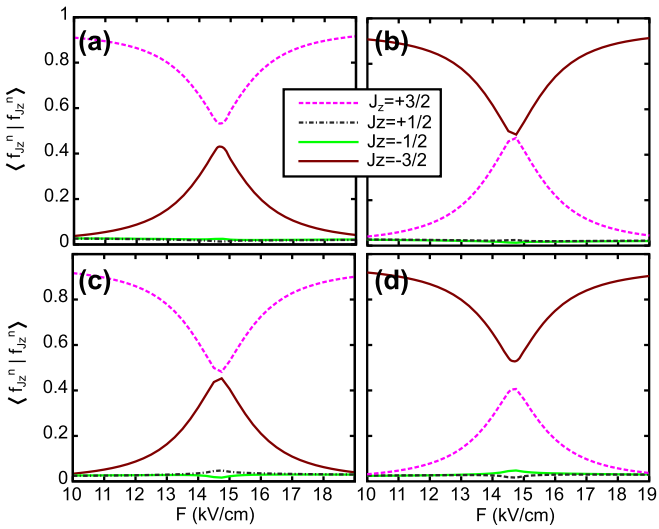

FIG. 2. (Color online) Weight of the different Luttinger spinor components of the hole states in Fig. 1(a), as a function of the electric field. Panels (a)–(d) correspond to states $|1\rangle$–$|4\rangle$, respectively. The states are almost exclusively HH ($J_z = \pm 3/2$).

where $f^n_{J_z}(\mathbf{r})$ is the envelope function associated with $|J = 3/2, J_z\rangle$, the periodic function with Bloch angular momentum J_z. $J_z = \pm 3/2$ correspond to spin-up and spin-down HH components, while $J_z = \pm 1/2$ correspond to LH components. The expectation value $\langle J_z\rangle = \sum_{J_z} J_z \langle f^n_{J_z}|f^n_{J_z}\rangle$ can be taken as a measure of the hole spin purity, with $\langle J_z\rangle \approx \pm 3/2$ indicating nearly pure HH spin-up ($\Uparrow$) or spin-down ($\Downarrow$) states.

For our calculations, we consider pyramidal $GaAs/Al_{0.3}Ga_{0.7}As$ QDMs with triangular confinement, similar to those obtained by metalorganic vapor deposition [26,27]. The vertically stacked QDs are separated by a barrier of thickness $d = 2$ nm, although they are interconnected by a thin $Al_{0.05}Ga_{0.95}As$ vertical quantum wire that enhances tunnel coupling; see the structure in Fig. 1(a) [33]. A weak magnetic field of $B = 0.2$ T is applied along the coupling direction. Figure 1(a) shows the energy of the first four hole states under the influence of a vertical electric field F. At $F = 11$ kV/cm we see two Zeeman-split doublets. The upper one (states $|1\rangle$ and $|2\rangle$) corresponds to the main component of the hole spinor in the top QD, which is slightly bigger than the bottom QD. In turn, the lower doublet (states $|3\rangle$ and $|4\rangle$) has the main component in the bottom dot. Since the increasing electric field favors the occupation of the bottom dot, a charge-transfer anticrossing takes place at $F = 14.7$ kV/cm (resonant electric field, F_r), where bonding and antibonding molecular orbitals are formed. The behavior closely resembles that of [001] grown QDMs [28,34,35], except for one anomaly: the Zeeman splitting of both doublets is quenched near the resonant electric field; see Fig. 1(a), inset.

The Zeeman splitting suppression can be seen as a vanishing effective g factor. Unlike in previous reports, however, the origin of this effect cannot be ascribed to the different g factor of the QD and barrier materials [36], as the QDs and the vertical wire connecting them have similar composition. Because electrically tunable g factors are of interest for spin manipulation [18], we further investigate into the origin of this phenomenon. Figure 1(b) shows the hole Bloch angular momentum expectation value of the four states under consideration. As can be seen, away from the resonant field, $\langle J_z\rangle$ gradually approaches $\pm 3/2$, indicating that the hole states confined in individual QDs are nearly HH states with fairly pure spin. In the vicinity of F_r, however, $\langle J_z\rangle \approx 0$, which means that for molecular states the spin becomes completely mixed.

For comparison, since [111] grown QDs normally have either a triangular or hexagonal shape [26,37,38], in Figs. 1(c) and 1(d) we study a QDM formed by hexagonal QDs. One can see that no spin mixing takes place near F_r in this case. Actually, the behavior is now the same as observed in vertically aligned [001] grown QDMs with C_{2h} symmetry QDs, where tunneling is a spin-preserving process [28]. It follows that the strong spin mixing in Fig. 1(b) is not a consequence of the [111] crystal orientation, but rather of the triangular envelope confinement. In fact, we also observe it for triangles grown along [001]; see the Supplemental Material [33]. It does not result from the presence or absence of strain either, as similar results are obtained using lattice mismatched materials such as InAs/GaAs [33]. Likewise, it is not induced by the magnetic field, as $\mathbb{H}_B$ is a diagonal term that does not couple different spinor component [33]. It does not take place in single QDs either. It is an exclusive property of QDMs with triangular confinement.

Further insight into the hole spin mixing mechanism is obtained in Fig. 2, which plots the weight of the four spinor components corresponding to each of the states $|1\rangle$–$|4\rangle$ of the triangular QDM. Two conclusions can be extracted: (i) LHs play a minor role in all cases, and the mixing is essentially between HH components with orthogonal spin projections ($J_z = \pm 3/2$); (ii) states $|1\rangle$ and $|4\rangle$ [panels (a) and (d)] seem to exhibit complementary behavior, and so do $|2\rangle$ and $|3\rangle$

[panels (b) and (d)]. This suggests that the spin mixing is due to independent interactions between $|1\rangle$ and $|4\rangle$ on the one hand, and $|2\rangle$ and $|3\rangle$ on the other.

To understand the origin of the HH spin mixing, we resort to a point group theory analysis. The Hamiltonian in Eq. (1) can be simplified as $\mathbb{H} \approx \mathbb{H}_{\rm LK}^{[111]} + \mathbb{H}_B + [V(\mathbf{r}) + e\,F\,z]\mathbb{I}$, where we have disregarded strain terms—which are weak for GaAs/AlAs heterostructures—and approximated $\mathbb{H}_{\rm BF}$ by the (constant mass) Luttinger-Kohn Hamiltonian:

$$\mathbb{H}_{\rm LK}^{[111]} = -\frac{1}{2}\begin{pmatrix} \hat{P}+\hat{Q} & -\hat{S} & \hat{R} & 0 \\ -\hat{S}^\dagger & \hat{P}-\hat{Q} & 0 & \hat{R} \\ \hat{R}^\dagger & 0 & \hat{P}-\hat{Q} & \hat{S} \\ 0 & \hat{R}^\dagger & \hat{S}^\dagger & \hat{P}+\hat{Q} \end{pmatrix} \tag{3}$$

with

$$\begin{aligned} \hat{P} \pm \hat{Q} &= (\gamma_1 \pm \gamma_3)\left(k_x^2 + k_y^2\right) + (\gamma_1 \mp 2\gamma_3)k_z^2, \\ \hat{R} &= -\frac{1}{\sqrt{3}}(\gamma_2 + 2\gamma_3)k_-^2 + \frac{2\sqrt{2}}{\sqrt{3}}(\gamma_2 - \gamma_3)k_+k_z, \\ \hat{S} &= -\frac{\sqrt{2}}{\sqrt{3}}(\gamma_2 - \gamma_3)k_+^2 + \frac{2}{\sqrt{3}}(2\gamma_2 + \gamma_3)k_-k_z, \end{aligned} \tag{4}$$

where $\gamma_1, \gamma_2, \gamma_3$ are the Luttinger parameters and $k_\pm = k_x \pm ik_y$. One can then see that $\mathbb{H}$ has C_3 point symmetry set by the confining potential $V(\mathbf{r})$. Near the resonant electric field, however, an additional approximate symmetry must be considered. Even if the two QDs forming the QDM are not identical, the electric field restores an *effective* parity symmetry, the bonding and antibonding HH molecular orbitals forming even and odd functions with respect to a mirror plane in between the QDs [34]. The corresponding point group is then C_{3h}. Note that for $\mathbb{H}_{\rm LK}^{[111]}$ to hold exact C_{3h} symmetry, we need to impose the so-called axial approximation ($\gamma_2 = \gamma_3$), which is actually valid for many III-V materials, such as GaAs. Actually, we do not impose exact symmetry in the numerical calculations, nevertheless the obtained results reveal, as expected, a high degree of symmetry.

The anticrossing of Fig. 1(a) can be rationalized considering the symmetry of the hole spinors in the double group $\bar{C}_{3h}$. Within this group, $|1\rangle$ and $|4\rangle$ have $E_{-3/2}$ symmetry, while $|2\rangle$ and $|3\rangle$ have $E_{3/2}$ symmetry [33]. The different symmetry of $|1\rangle$ and $|2\rangle$ ($|3\rangle$ and $|4\rangle$) explains the lack of interaction within the Zeeman doublets, in spite of the quasidegeneracy. It also becomes clear why $|1\rangle$ and $|4\rangle$ ($|2\rangle$ and $|3\rangle$) interact separately, as observed in Fig. 2.

The above picture differs from the widely studied [001] grown QDMs with circular confinement, where the symmetry of all four spinorial states involved in the molecular anticrossing is different [34], which results in the absence of interaction and hence spin-preserving tunneling. Sizable hole spin mixing has been observed only in QDMs with significant misalignment [30], because the symmetry is then completely reduced ($\bar{C}_1$ point group). Nevertheless, the largest spin anticrossing measured for such a system is 0.4 meV, corresponding to InAs QDMs with anomalously large lateral offset [25]. This is 2.5 times smaller than the 1 meV gap we estimate in Fig. 1, and 6 times smaller than the 2.5 meV we predict for InAs/GaAs QDMs [33].

To explain the unusual strength of the spin-orbit coupling in triangular QDMs, we can examine the envelope symmetry of $\mathbb{H}_{\rm LK}^{[111]}$ (within an axial approximation) and the ensuing eigenfunctions. In the C_{3h} point group, the terms of Eq. (3) form the basis of the following irreducible representations:

$$\Gamma_{H_{\rm LK}} = \begin{pmatrix} A' & E_-'' & E_+' & 0 \\ E_+'' & A' & 0 & E_+' \\ E_-' & 0 & A' & E_-'' \\ 0 & E_-' & E_+'' & A' \end{pmatrix}. \tag{5}$$

A remarkable consequence is that for any hole state $|n\rangle$, the envelope functions of the spin-up and -down HH components, $f_{3/2}^n$ and $f_{-3/2}^n$ in Eq. (2), must have the same symmetry except for the even/odd parity (e.g., A' and A''). This is a key factor in determining the strength of the spin admixture, as we show in the perturbative analysis below.

Hamiltonian $\mathbb{H}$ can be split as a sum of diagonal and off-diagonal terms, $\mathbb{H} = \mathbb{H}_0 + \mathbb{H}'$, the latter being responsible for band coupling. If we disregard $\mathbb{H}'$, the levels anticrossing at F_r are those represented at the top of Fig. 3(a), namely two Zeeman doublets formed by HHs with opposite spin ($J_z = \pm 3/2$) but the same rotational symmetry (A) and parity ($'$ or $''$). Each doublet is split by a Zeeman term Δ_B^0 and separated from each other by an amount $2t$, where t is the HH tunneling integral. Considering $\mathbb{H}'$ as a perturbative term, the mixing between the spin-up ground state $|k^{(0)}\rangle = (A', +3/2)$ and any spin-down HH state $|i^{(0)}\rangle$ is given by

$$|k^{(2)}\rangle = \sum_{i\neq k}\left(\sum_{j\neq k}\frac{\langle i^{(0)}|\mathbb{H}'|j^{(0)}\rangle}{E_k^0 - E_i^0}\frac{\langle j^{(0)}|\mathbb{H}'|k^{(0)}\rangle}{E_k^0 - E_j^0}\right)|i^{(0)}\rangle, \tag{6}$$

where $|j^{(0)}\rangle$ is the jth intermediate state and E_j^0 is its corresponding energy. Notice that the strength of coupling is inversely proportional to $\Delta E_{\rm hh} = E_k^0 - E_i^0$, i.e., the energy difference between the spin-up and -down HH states. As explained in detail in the Supplemental Material [33], the symmetry of $\mathbb{H}'$ operators, off-diagonal terms of Eq. (5), translates into selection rules that make the numerator of Eq. (6) vanish for all except the two paths plotted with thick arrows in Fig. 3(a). Both paths involve excited LHs as intermediate states [39], and the spin-down HH is $|i\rangle = (A'', -3/2)$, i.e., a state participating in the molecular anticrossing. This implies $\Delta E_{\rm hh}$ is small (a few meV at most), and is in contrast with other point symmetries, where selection rules lead to coupling with higher excited HH states, so that $\Delta E_{\rm hh}$ is much larger. For example, if we consider QDMs with circular QDs (point group $C_{\infty h}$), the HH components coupled by $\mathbb{H}'$ no longer have the same rotational symmetry, but they differ by three quanta of azimuthal angular momentum M_z [34]. Consequently, there is no coupling between the $M_z = 0$ HHs forming the molecular anticrossing [33]. Having a QDM structure is also essential, as then A' and A'' are roughly split by the tunneling energy $2t$, which can be made small enough for the SOI to be efficient. By contrast, in single QDs the strong vertical confinement would lead to several meV splitting.

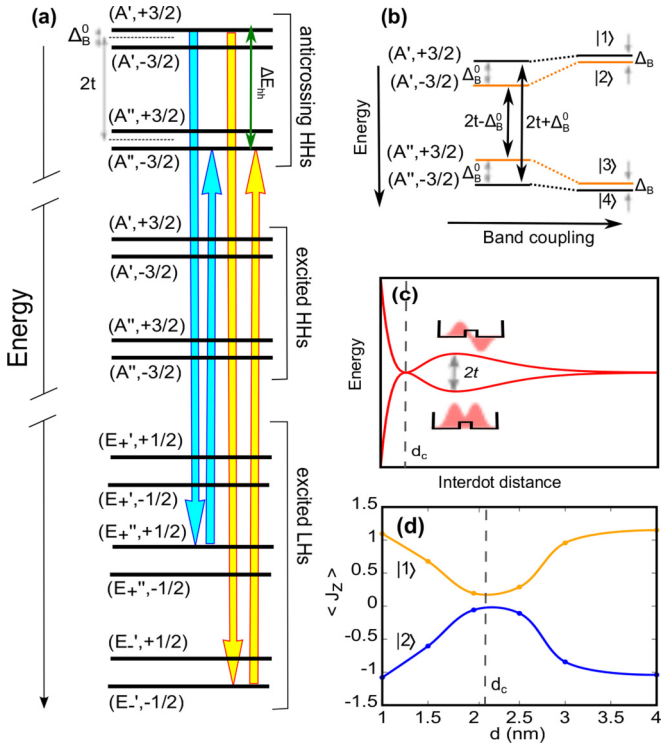

FIG. 3. (Color online) (a) Diagram of single-band hole energy levels under a longitudinal magnetic field for a QDM with symmetry C_{3h}. The labels (X^p, J_z) indicate the symmetry of the levels. X represents the rotational symmetry of the envelope function (A, $E_\pm$) while $p = \prime$ or $\prime\prime$ represents the even/odd parity and J_z indicates the nonzero component of the spinor. Thick arrows denote the symmetry-allowed level couplings for the ground state. (b) Energy structure of anticrossing hole states before and after switching on off-diagonal terms in $\mathbb{H}_{\mathrm{LK}}^{[111]}$. (c) Typical dissociation energy spectrum of holes in QDMs at $B = 0$ T, showing a bonding-antibonding ground-state reversal at d_c. (d) Calculated spin purity of states $|1\rangle$ and $|2\rangle$ for different interdot distances at the resonant electric field. Spin mixing is strongest around d_c.

The suppression of the Zeeman splitting observed in Fig. 1(a) can also be understood from the perturbative analysis. As indicated in Fig. 3(b), the band coupling occurs between HH states belonging to different doublets. Because ΔE_{hh} is smaller for the innermost states $(2t - \Delta_B^0)$ than for the outermost ones $(2t + \Delta_B^0)$, the interaction is stronger, leading to an effectively reduced Zeeman splitting, Δ_B.

It is clear from the discussions above that tunneling must be an important parameter to control the strength of the spin mixing. One might then expect that spin mixing is enhanced for long interdot distances d, when tunneling energy t is small. Figure 3(d) shows the spin purity of the ground-state HH for QDMs with different d at resonant electric field. Interestingly, the maximum spin mixing is found at intermediate distances, $d \approx 2$ nm. This follows from the characteristic, nonmonotonous decay of hole tunneling in QDMs [34,35,40,41]. As shown in the schematic of Fig. 3(c), there is a critical distance d_c where bonding and antibonding hole states are reversed. At this point, t has a relative minimum combined with large wave-function delocalization, which enables the strong spin mixing. For $d < d_c$, t increases rapidly, reducing the interaction. For $d > d_c$, t eventually decreases, but so does the wave-function delocalization. As a result, we gradually retrieve the single QD limit, were spin mixing is weak.

Electrical control of hole spins in QDMs has been proposed as a key ingredient for scalable qubit architectures [25]. So far, however, only [001] grown QDMs have been considered, where the main source of spin mixing was misalignment between the vertically stacked dots [30], which is a difficult parameter to regulate experimentally. The C_{3h}-symmetry-induced spin mixing described here arises as a more robust and manageable mechanism. It can also help increase the fidelity of spin control gate operations, as this requires the spin mixed states to (i) be energetically well resolved, and (ii) be able to form indirect excitons with large optical dipole strength [25]. As for (i), we predict strong mixing between states 1 meV away from each other, larger than any previous measurement. As for (ii), unlike in misaligned QDMs, the spin mixing we describe is strong at the resonant electric field, where direct and indirect excitons have comparable optical strength. Another advantage is the possibility to use weak magnetic fields, which limits the influence of the g-factor inhomogeneity of different QDs in the qubit scaling.

In summary, we have shown that triangular QDs can be used to build QDMs with electrically controllable hole spin. The hole spin is well defined inside the individual QDs, but the formation of delocalized molecular orbitals with C_{3h} symmetry enables SOI-induced mixing with unprecedented strength. The reversible control, the strength of the interaction, and the robust nature of the spin-mixing mechanism imply that holes in triangular QDMs, like those obtained with [111] growth, form a promising system for quantum-information processing with some advantages as compared to circular [001] grown QDMs.

Support from Universitat Jaume I (UJI) project P1-1B2014-24 and MINECO project CTQ2014-60178-P is acknowledged.

[1] C. Kloeffel and D. Loss, Prospects for spin-based quantum computing in quantum dots, Annu. Rev. Condens. Matter Phys. **4**, 51 (2013).

[2] R. J. Warburton, Single spins in self-assembled quantum dots, Nat. Mater. **12**, 483 (2013).

[3] K. De Greve, D. Press, P. L. McMahon, and Y. Yamamoto, Ultrafast optical control of individual quantum dot spin qubits, Rep. Prog. Phys. **76**, 092501 (2013).

[4] A. J. Ramsay, A. review of the coherent optical control of the exciton and spin states of semiconductor quantum dots, Semicond. Sci. Technol. **25**, 103001 (2010).

[5] R. Dahbashi, J. Huebner, F. Berski, K. Pierz, and M. Oestreich, Optical spin noise of a single hole spin localized in an (InGa)As quantum dot, Phys. Rev. Lett. **112**, 156601 (2014).

[6] J. Houel, J. H. Prechtel, A. V. Kuhlmann, D. Brunner, C. E. Kuklewicz, B. D. Gerardot, N. G. Stoltz, P. M. Petroff, and

R. J. Warburton, High resolution coherent population trapping on a single hole spin in a semiconductor quantum dot, Phys. Rev. Lett. **112**, 107401 (2014).

[7] X. J. Wang, S. Chesi, and W. A. Coish, Spin-echo dynamics of a heavy hole in a quantum dot, Phys. Rev. Lett. **109**, 237601 (2012).

[8] F. Fras, B. Eble, P. Desfonds, F. Bernardot, C. Testelin, M. Chamarro, A. Miard, and A. Lemaitre, Hole-spin initialization and relaxation times in InAs/GaAs quantum dots, Phys. Rev. B **84**, 125431 (2011).

[9] D. Heiss, S. Schaeck, H. Huebl, M. Bichler, G. Abstreiter, J. J. Finley, D. V. Bulaev, and D. Loss, Observation of extremely slow hole spin relaxation in self-assembled quantum dots, Phys. Rev. B **76**, 241306 (2007).

[10] K. Mueller, A. Bechtold, C. Ruppert, C. Hautmann, J. S. Wildmann, T. Kaldewey, M. Bichler, H. J. Krenner, G. Abstreiter, M. Betz, and J. J. Finley, High-fidelity optical preparation and coherent Larmor precession of a single hole in an (In,Ga)As quantum dot molecule, Phys. Rev. B **85**, 241306 (2012).

[11] T. M. Godden, J. H. Quilter, A. J. Ramsay, Yanwen Wu, P. Brereton, S. J. Boyle, I. J. Luxmoore, J. Puebla-Nunez, A. M. Fox, and M. S. Skolnick, Coherent optical control of the spin of a single hole in an InAs/GaAs quantum dot, Phys. Rev. Lett. **108**, 017402 (2012).

[12] T. M. Godden, J. H. Quilter, A. J. Ramsay, Y. Wu, P. Brereton, I. J. Luxmoore, J. Puebla, A. M. Fox, and M. S. Skolnick, Fast preparation of a single-hole spin in an InAs/GaAs quantum dot in a Voigt-geometry magnetic field, Phys. Rev. B **85**, 155310 (2012).

[13] A. Greilich, S. G. Carter, D. Kim, A. S. Bracker, and D. Gammon, Optical control of one and two hole spins in interacting quantum dots, Nat. Photon. **5**, 703 (2011).

[14] P. Szumniak, S. Bednarek, B. Partoens, and F. M. Peeters, Spin-orbit-mediated manipulation of heavy-hole spin qubits in gated semiconductor nanodevices, Phys. Rev. Lett. **109**, 107201 (2012).

[15] J. C. Budich, D. G. Rothe, E. M. Hankiewicz, and B. Trauzettel, All-electric qubit control in heavy hole quantum dots via non-Abelian geometric phases, Phys. Rev. B **85**, 205425 (2012).

[16] J. Pingenot, C. E. Pryor, and M. E. Flatte, Electric-field manipulation of the Lande g tensor of a hole in an $In_{0.5}Ga_{0.5}As$/GaAs self-assembled quantum dot, Phys. Rev. B **84**, 195403 (2011).

[17] V. Jovanov, T. Eissfeller, S. Kapfinger, E. C. Clark, F. Klotz, M. Bichler, J. G. Keizer, P. M. Koenraad, G. Abstreiter, and J. J. Finley, Observation and explanation of strong electrically tunable exciton g factors in composition engineered In(Ga)As quantum dots, Phys. Rev. B **83**, 161303 (2011).

[18] M. F. Doty and D. Gammon, Getting a handle on spin, Physics **2**, 16 (2009).

[19] T. M. Godden, S. J. Boyle, A. J. Ramsay, A. M. Fox, and M. S. Skolnick, Fast high fidelity hole spin initialization in a single InGaAs quantum dot, Appl. Phys. Lett. **97**, 061113 (2010).

[20] K. F. Karlsson, M. A. Dupertuis, D. Y. Oberli, E. Pelucchi, A. Rudra, P. O. Holtz, and E. Kapon, Fine structure of exciton complexes in high-symmetry quantum dots: Effects of symmetry breaking and symmetry elevation, Phys. Rev. B **81**, 161307 (2010).

[21] R. Singh and G. Bester, Nanowire quantum dots as an ideal source of entangled photon pairs, Phys. Rev. Lett. **103**, 063601 (2009).

[22] K. F. Karlsson, V. Troncale, D. Y. Oberli, A. Malko, E. Pelucchi, A. Rudra, and E. Kapon, Optical polarization anisotropy and hole states in pyramidal quantum dots, Appl. Phys. Lett. **89**, 251113 (2006).

[23] G. Sallen, B. Urbaszek, M. M. Glazov, E. L. Ivchenko, T. Kuroda, T. Mano, S. Kunz, M. Abbarchi, K. Sakoda, D. Lagarde, A. Balocchi, X. Marie, and T. Amand, Dark-bright mixing of interband transitions in symmetric semiconductor quantum dots, Phys. Rev. Lett. **107**, 166604 (2011).

[24] A. N. Vamivakas, C. Y. Lu, C. Matthiesen, Y. Zhao, S. Falt, A. Badolato, and M. Atatuere, Observation of spin-dependent quantum jumps via quantum dot resonance fluorescence, Nature (London) **467**, 297 (2010).

[25] S. E. Economou, J. I. Climente, A. Badolato, A. S. Bracker, D. Gammon, and M. F. Doty, Scalable qubit architecture based on holes in quantum dot molecules, Phys. Rev. B **86**, 085319 (2012).

[26] Q. Zhu, K. F. Karlsson, M. Byszewski, A. Rudra, E. Pelucchi, Z. He, and E. Kapon, Hybridization of electron and hole states in semiconductor quantum-dot molecules, Small **5**, 329 (2009).

[27] F. Michelini, M. A. Dupertuis, and E. Kapon, Novel artificial molecules: Optoelectronic properties of two quantum dots coupled by a quantum wire, in *Proceedings of the 14th International Workshop on Computational Electronics* (IEEE, New York, 2010), p. 255.

[28] E. A. Stinaff, M. Scheibner, A. S. Bracker, I. V. Ponomarev, V. L. Korenev, M. E. Ware, M. F. Doty, T. L. Reinecke, and D. Gammon, Optical signatures of coupled quantum dots, Science **311**, 636 (2006).

[29] R. Winkler, *Spin-orbit Coupling Effects in Two-dimensional Electron and Hole Systems* (Springer-Verlag, Berlin, 2003).

[30] M. F. Doty, J. I. Climente, A. Greilich, M. Yakes, A. S. Bracker, and D. Gammon, Hole-spin mixing in InAs quantum dot molecules, Phys. Rev. B **81**, 035308 (2010).

[31] B. A. Foreman, Effective-mass Hamiltonian and boundary conditions for the valence bands of semiconductor microstructures, Phys. Rev. B **48**, 4964 (1993).

[32] J. M. Luttinger, Quantum theory of cyclotron resonance in semiconductors: General theory, Phys. Rev. **102**, 1030 (1956).

[33] See supplemental material at http://link.aps.org/supplemental/10.1103/PhysRevB.92.041302 for model details, parameters, double group tables, and supporting calculations.

[34] J. I. Climente, M. Korkusinski, G. Goldoni, and P. Hawrylak, Theory of valence-band holes as Luttinger spinors in vertically coupled quantum dots, Phys. Rev. B **78**, 115323 (2008).

[35] M. F. Doty, J. I. Climente, M. Korkusinski, M. Scheibner, A. S. Bracker, P. Hawrylak, and D. Gammon, Antibonding ground states in InAs quantum-dot molecules, Phys. Rev. Lett. **102**, 047401 (2009).

[36] M. F. Doty, M. Scheibner, I. V. Ponomarev, E. A. Stinaff, A. S. Bracker, V. L. Korenev, T. L. Reinecke, and D. Gammon, Electrically tunable g factors in quantum dot molecular spin states, Phys. Rev. Lett. **97**, 197202 (2006).

[37] M. Jo, T. Mano, M. Abbarchi, T. Kuroda, Y. Sakuma, and K. Sakoda, Self-limiting growth of hexagonal and triangular quantum dots on (111)A, Cryst. Growth Des. **12**, 1411 (2012).

[38] A. Pfund, I. Shorubalko, R. Leturcq, and K. Ensslin, Top-gate defined double quantum dots in InAs nanowires, Appl. Phys. Lett. **89**, 252106 (2006).

[39] $\mathbb{H}'$ has no term mixing spin up and down HH directly. The mixing is mediated by LH through $\hat{R}$ and $\hat{S}$ operators. Thus, the spin admixture we report is proportional to the Luttinger parameters γ_2 and γ_3. Since the value of these parameters is modulated by the strength of the spin-orbit interaction, the extent of the spin admixture is ultimately due to spin-orbit interaction.

[40] W. Jaskolski, M. Zielinski, Garnett W. Bryant, and J. Aizpurua, Strain effects on the electronic structure of strongly coupled self-assembled InAs/GaAs quantum dots: Tight-binding approach, Phys. Rev. B **74**, 195339 (2006).

[41] G. Bester, J. Shumway, and A. Zunger, Theory of excitonic spectra and entanglement engineering in dot molecules, Phys. Rev. Lett. **93**, 047401 (2004).